Research Article Vol. 30, No. 5 / 28 Feb 2022 / Optics Express 7044
Optics EXPRESS

Hollow-core fiber delivery of broadband mid-infrared light for remote spectroscopy

KERR JOHNSON,[1] PABLO CASTRO-MARIN,[2] CARL FARRELL,[1] IAN A. DAVIDSON,[3] QIANG FU,[3] GREGORY T. JASION,[3] NATALIE V. WHEELER,[3] FRANCESCO POLETTI,[3] DAVID J. RICHARDSON,[3] AND DERRYCK T. REID[2,*]

[1]*Chromacity Ltd, Livingstone House, 43 Discovery Terrace, Research Avenue North, Riccarton, Edinburgh, EH14 4AP, UK*
[2]*School of Engineering and Physical Sciences, Heriot–Watt University, Edinburgh, EH14 4AS, UK*
[3]*Optoelectronics Research Centre, Zepler Institute of Photonics and Nanoelectronics, University of Southampton, Southampton, SO17 1BJ, UK*
[*]*D.T.Reid@hw.ac.uk*

Abstract: High-resolution multi-species spectroscopy is achieved by delivering broadband 3–4-μm mid-infrared light through a 4.5-meter-long silica-based hollow-core optical fiber. Absorptions from $H^{37}Cl$, $H^{35}Cl$, H_2O and CH_4 present in the gas within the fiber core are observed, and the corresponding gas concentrations are obtained to 5-ppb precision using a high-resolution Fourier-transform spectrometer and a full-spectrum multi-species fitting algorithm. We show that by fully fitting the narrow absorption features of these light molecules their contributions can be nulled, enabling further spectroscopy of C_3H_6O and C_3H_8O contained in a Herriott cell after the fiber. As a demonstration of the potential to extend fiber-delivered broadband mid-infrared spectroscopy to significant distances, we present a high-resolution characterization of the transmission of a 63-meter length of hollow-core fiber, fully fitting the input and output spectra to obtain the intra-fiber gas concentrations. We show that, despite the fiber not having been purged, useful spectroscopic windows are still preserved which have the potential to enable hydrocarbon spectroscopy at the distal end of fibers with lengths of tens or even hundreds of meters.

1. Introduction

Hollow-core fibers (HCFs) are a specialty optical fiber where light is guided within a (usually) air-filled core. Low-loss light transmission is enabled by a carefully designed microstructure, formed from thin silica membranes surrounding the hollow core. Compared to conventional optical fibers, where light is guided within a solid glass core, HCFs can provide several advantages, including ultimate low latency and ultralow nonlinearity. HCFs are also an exciting candidate for mid-infrared (mid-IR) applications as the extremely low overlap between the guided light and the silica microstructure enables low-loss propagation significantly beyond the transmission cut-off of bulk silica. Several low-loss mid-IR HCFs have been reported [1,2,3], and recently HCFs with attenuation as low as 18 dB km^{-1} at 3.1 μm were demonstrated [4], underlining the potential of this technology in this spectral region. The relatively high fiber yields achievable are also an advantage compared to other mid-IR fibers (such as ZrF_4), as they enable fabrication of potentially multi-kilometer lengths of HCF. An additional interesting property of HCFs is that the core can be filled with gas to provide an extremely long optical interaction length, within a compact footprint (the fibers can be coiled), while requiring only a very small gas volume (~μL). This can be exploited for both nonlinear optics and sensing applications, the latter being

#450413 https://doi.org/10.1364/OE.450413
Journal © 2022 Received 7 Dec 2021; revised 19 Jan 2022; accepted 19 Jan 2022; published 16 Feb 2022

Optics EXPRESS

especially promising for mid-IR gas detection, as the mid-IR spectral region overlaps with the fingerprint absorption features of many gases of interest within environmental and industrial monitoring applications.

While the first reports into the potential of HCFs for gas detection focused on the near-IR [5], the emergence of low-loss mid-IR HCFs has motivated several investigations in this spectral region. Early reports used hollow-core photonic bandgap fibers (HC-PBGFs); in 2008, Gayraud [6] reported detection of methane gas with an estimated limit of detection of 50 ppm using an OPO light source combined with a Fourier-transform spectroscopy detection scheme. Later, in 2014, Petrovich [7] reported a 0.9-ppm limit of detection for ethane using a supercontinuum source and optical spectrum analyzer for detection. In these demonstrations, the ultimate sensitivity was limited by modal interference, as higher order modes can be guided in HC-PBGFs with low loss. More recently, there have been several reports of mid-IR gas sensing using hollow-core anti-resonant fibers (HC-ARFs) [8,9,10,11,12,13]; this fiber design can provide key advantages for gas detection, including effectively single-mode transmission (depending on design, launch conditions and fiber length) which reduces modal interference effects, and a larger core diameter, which reduces gas filling time. Additionally, HC-ARFs provide broadband guidance across multiple transmission windows, and the most recent designs (with 'non-contact' cladding structures, following [1]) enable low loss across these transmission windows, free from spectrally localized regions of increased loss due to structural resonances. Using a quantum cascade laser operating at 4.53 μm, wavelength modulation spectroscopy and a 3.2-m length of tubular HC-ARF, Nikodem [11] recently reported a limit of detection of 5.4 ppbv for nitrous oxide. However, nearly all reports are limited to single species gas detection, excluding [12] where both carbon dioxide and methane were detected using the same fiber.

Here, we report an alternative approach and explore the capabilities of HC-ARFs for both multi-species gas detection and beam delivery over long fiber lengths in the 3.0–3.5-μm spectral region. By combining broadband illumination with high-resolution Fourier-transform spectroscopy we obtain simultaneous concentrations of $H^{37}Cl$, $H^{35}Cl$, H_2O and CH_4 trapped in the HCF core, and do so with 5-ppb precision for the HCl isotopologues and CH_4, whose concentrations are sufficiently stable to permit averaging. HCl is a common contaminant associated with the use of chlorine for dehydration in the glass production process and has previously been measured in the internal gas composition of HCFs fabricated from F300 glass [3,14,15]. Previous mitigation measures have included purging the fiber with an inert gas to remove the HCl [3] but this is not always practical, and it is not guaranteed that the HCl features will not return in time. Here we show how the spectroscopic impact of these line-like absorbers can be mitigated by using high-resolution spectroscopy, allowing further concentration measurements of additional molecules to be made in a gas cell situated after the HCF. As a final demonstration of a pathway to fiber-delivered mid-IR spectroscopy over significant distances we characterize the spectra before and after a 63-m HCF, showing that clear spectroscopic windows exist which are unaffected by intra-fiber absorptions and that would be suitable for remote hydrocarbon spectroscopy.

2. Hollow-core fiber fabrication and performance

The fiber used in this work was fabricated using Heraeus F300 fused silica glass and the conventional stack and draw process. In this method, a series of capillaries is first stacked to form a macroscopic preform, which is then fused and drawn to ~3-mm canes, and finally these canes are jacketed and drawn to fiber [16]. During the fiber drawing stage, multi-zone pressurization and inline fluid-dynamic modelling are used to achieve the desired structure and ensure meaningful yields [16]. The fiber was designed to operate with a fundamental transmission window in the mid-IR, in particular overlapping with the 3.0–3.5 μm wavelength range relevant for the gas sensing work presented here. The preform design used allows fiber lengths exceeding 1 km to be collected, but in this case a series of shorter, structurally different bands was prioritized.

Optics EXPRESS

The band we report in this work was originally ~70 m in length, however we have successfully collected mid-IR guiding bands over 300 m in length which could be readily extended.

Figure 1(a) shows a scanning electron microscope (SEM) image of the fiber cross-section recorded using a Phenom ProX desktop SEM, a charge reducing mount and a 10-kV electron beam voltage. Based on this image, the fiber has a 77-μm core, 51.0 ± 1.0 μm diameter cladding tubes, 5.2 ± 1.3 μm inter-tube gaps, and 930 ± 30 nm tube membrane thicknesses. The fiber's excellent optical properties are attributed to the small variation in its structural parameters.

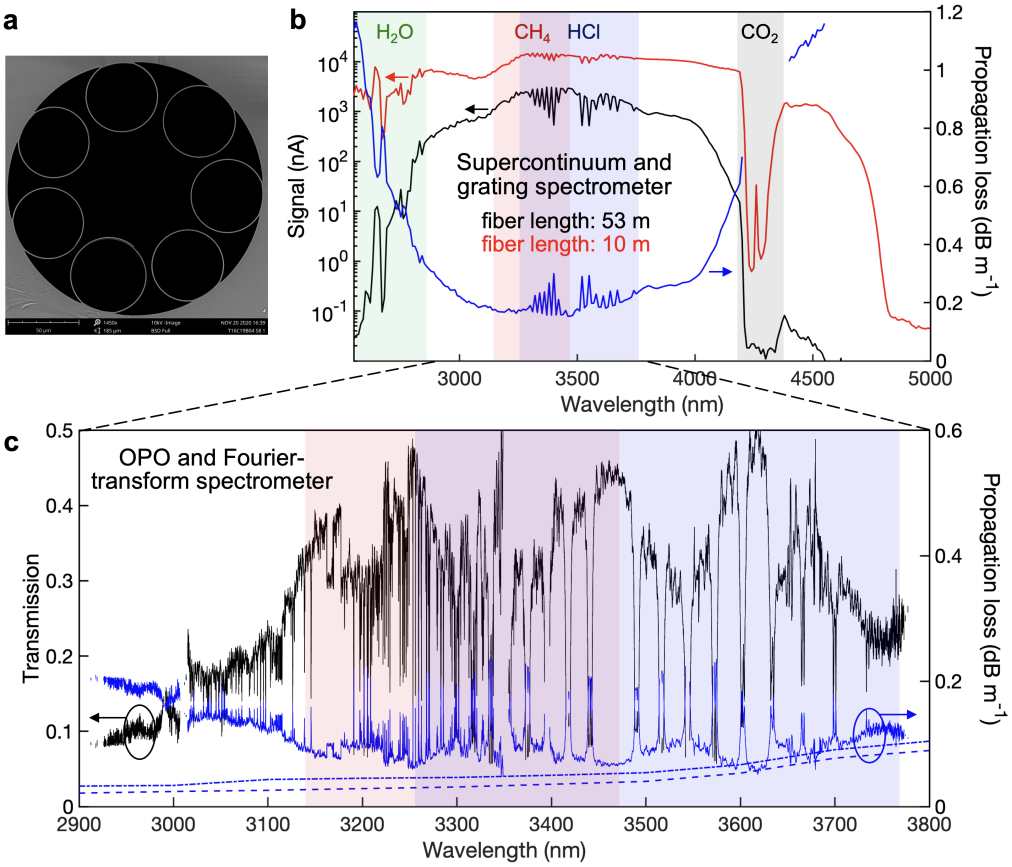

Fig. 1. (a) SEM image of the fiber cross-section. (b) Transmission of 10-m (red) and 53-m (black) fiber lengths measured using a super-continuum source and a grating spectrometer (10-nm measurement resolution). The computed loss is shown in blue. (c) High-resolution transmission spectrum inferred from a cut-back measurement from 63 m to 10 m (black) and corresponding loss (blue, solid). The simulated fiber loss is also shown (straight: dashed; and with 30-cm bend diameter: dash-dotted curves. Parasitic absorption from H_2O, HCl, CH_4 (weakly) and CO_2 trapped in the fiber core is responsible for the higher loss features in the shaded spectral regions.

In Fig. 1(b) we present fiber attenuation measurements obtained using the cut-back technique, where a long length of the HCF was cut back to 10 m while maintaining a consistent launch. For both fiber lengths, the fiber was coiled to a diameter of ~30 cm. In an initial low-resolution survey, Fig. 1(b), we used a supercontinuum source (Leukos Electro MIR 4.8) and a grating spectrometer to obtain the propagation loss by recording broadband transmission spectra from 1–5 μm at a spectral resolution of 10 nm, first for a 53-m length, and then, after cutting this

Optics EXPRESS

back, a length of 10 m. The results show a minimum loss of around 0.15 dB m^{-1}, occurring in the spectral region between ~3.2 μm and 3.5 μm, yet this spectral range also contains strong absorption lines from the $H^{35}Cl$ and $H^{37}Cl$ present inside the fiber core.

The limited spectral resolution of the grating-spectrometer may fail to resolve the low-loss regions between strong molecular absorption lines. To address this, we used an OPO source and Fourier-transform spectrometer (described in detail in Section 3) to perform a high-resolution (~0.05 cm^{-1}) cut-back measurement from 63 m to 10 m. The results are shown in Fig. 1(c), and reveal strong contributions from both CH_4 and HCl, which dominate the spectrum. Using high-resolution allows us to fully resolve the loss in the regions between molecular absorption lines and to compare this with the simulated waveguide loss. In Fig. 1(c), the dashed and dash-dotted lines are the fiber loss simulated in COMSOL, for straight and 30 cm coil diameter fibers respectively. These show that the performance of the fiber approaches the theoretical transmission in regions where there is no in-fiber gas absorption.

In the remainder of this paper we introduce an implementation of high-resolution Fourier-transform spectroscopy. This firstly allows us to characterize the path-integrated concentrations of absorbers present inside the HCF, such as H_2O, CH_4 and HCl, which are normally present in the core of the fiber due to atmospheric ingress and, in the case of HCl, the raw material used to fabricate the fiber (F300 from Heraeus). This demonstrates the potential of the technique used here for in-fiber gas sensing. Then, we show that, by using sufficiently high-resolution spectroscopy, these species need not prevent the fiber being used as a delivery channel for remote, multi-species hydrocarbon spectroscopy, even when purging them from the fiber core is not possible.

3. High-resolution spectroscopy configuration

The spectroscopy arrangement is illustrated in Fig. 2. Spectroscopy was performed using a commercial ultrafast optical parametric oscillator (OPO) from Chromacity Ltd. and a Fourier-transform spectrometer similar to that reported elsewhere [17,18]. The OPO produced >150-fs

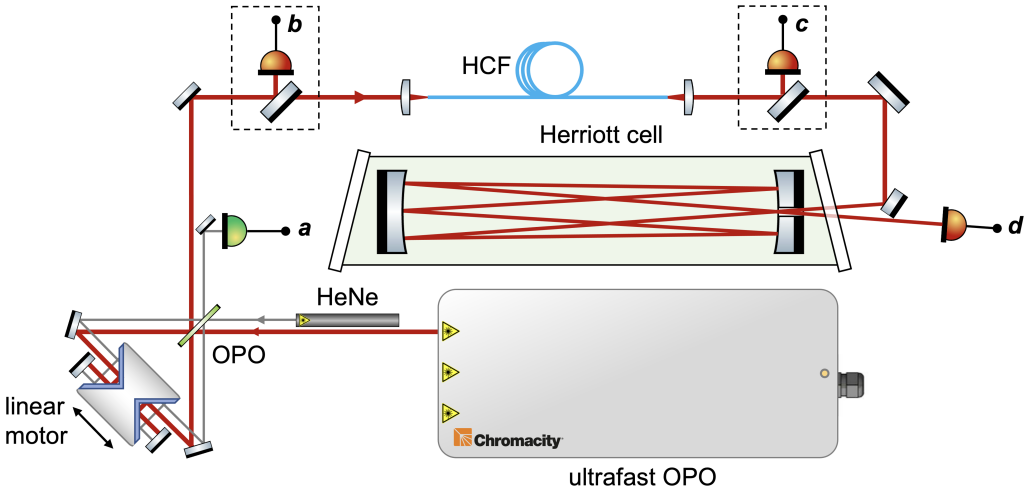

Fig. 2. OPO spectrometer and gas cell. Light from the OPO is routed through a scanning Michelson interferometer before being coupled into the delivery fiber. Calibration fringes (detector *a*) from a HeNe laser are recorded in synchronism with the mid-IR interferogram recorded either immediately before (detector *b*) or after (detector *c*) the fiber, or after a gas cell situated at the fiber output (detector *d*). Detector *a* was a silicon photodiode; all others were thermo-electrically cooled InAsSb amplified detectors.

Optics EXPRESS

idler pulses at a 300-MHz repetition rate, which were centered at a wavelength of 3.3 μm with an instantaneous bandwidth of around 200 nm and produced an average power in this wavelength band of up to 300 mW. The center wavelength of the OPO was tunable from 2.9–3.8 μm, enabling spectroscopy across this region.

Light from the OPO entered a Michelson interferometer scanning at 1 Hz and that provided interferograms with an optical path difference of up to 40 cm, corresponding to a wavenumber resolution approaching 0.025 cm^{-1}. In air at ambient temperature and pressure, this resolution is sufficient to clearly resolve the rovibrational absorption lines of many light molecules. The optical path difference was calibrated by co-injecting light from a 632.8-nm HeNe laser into the interferometer and recording fringes from this (detector *a* in Fig. 2) on a digitizer synchronously with OPO interferograms measured either immediately before (detector *b* in Fig. 2) or after (detector *c* in Fig. 2) the HCF, or after a Herriott cell placed at the HCF output (detector *d* in Fig. 2). The Herriott cell was a Thorlabs HC10L/M-M02, with an effective path length of 10.5 m and 28 internal reflections. A fringe-counting algorithm used the HeNe fringes to impose a precision delay axis on the mid-infrared interferograms, allowing them to be Fourier-transformed to yield high-resolution spectra. These spectra were processed to remove étalon artefacts as described in [19] before being fitted [17,20] to absorption data from the HITRAN database [21,22] (for all compounds except isopropanol, which was sourced from the PNNL database [23]).

4. Demonstration of HCF-delivered gas-cell spectroscopy

Using a 4.5-meter length of HCF we recorded spectra after the Herriott cell, into which additional absorbers could be introduced. This arrangement allowed us to assess the impact on the gas-cell spectroscopy of the absorption features already present from HCl, water vapor and methane contained in the HCF delivery fiber. In Fig. 3(a) we present an average of 200 spectra recorded when the Herriott cell contained only ambient air. Using a full-spectrum minimization approach, the spectra were fitted by a procedure [17,20] that simultaneously extracts (as a multi-point spline) the effective spectral illumination envelope of the light and the concentrations of the participating species. Inside the HCF, water and methane are present in near-ambient concentrations, but there is also strong absorption from $H^{37}Cl$ and $H^{35}Cl$. These species are a contaminant associated with the use of chlorine for dehydration in the glass production process and give rise to the strong pairs of lines that can be seen across the spectrum in their naturally occurring isotopic fraction. In a later experiment, we recorded 1000 consecutive spectra at 6-second intervals (no averaging) and independently processed each using the same fitting procedure to obtain values for H_2O, CH_4 and HCl concentrations, as presented in Fig. 3(c). Water (H_2O) and methane (CH_4) were detected at average concentrations of ~0.6% and 2 ppm respectively. The average HCl content in the core of this fiber was measured as 3.6 ppm. The measurement of H_2O showed a small systematic change (±0.03%) during the course of the measurements (~100 minutes), which we attribute to ambient environmental changes, but the CH_4 and HCl concentrations showed a near-random variation. An Allan deviation analysis made using these data (Fig. 3(d)) showed that averaging over 256 samples was effective in improving the precision to a level of ~5 ppb for both CH_4 and HCl.

As a demonstration of hydrocarbon spectroscopy after light delivery via the HCF we introduced small amounts of isopropanol (IPA, C_3H_8O) and acetone (C_3H_6O) vapor into the Herriott cell and repeated the measurements. The resulting spectrum is shown in Fig. 3(b). The measured concentrations were 237 ppm for acetone and 39.3 ppm for isopropanol, consistent with the volume of liquid acetone and isopropanol introduced. Here, the fitting procedure was constrained using the illumination spectrum measured before the HCF (see [17] for a full description of this method) to avoid the broadband continuum-like features of isopropanol and acetone being erroneously fitted into the illumination envelope.

Optics EXPRESS

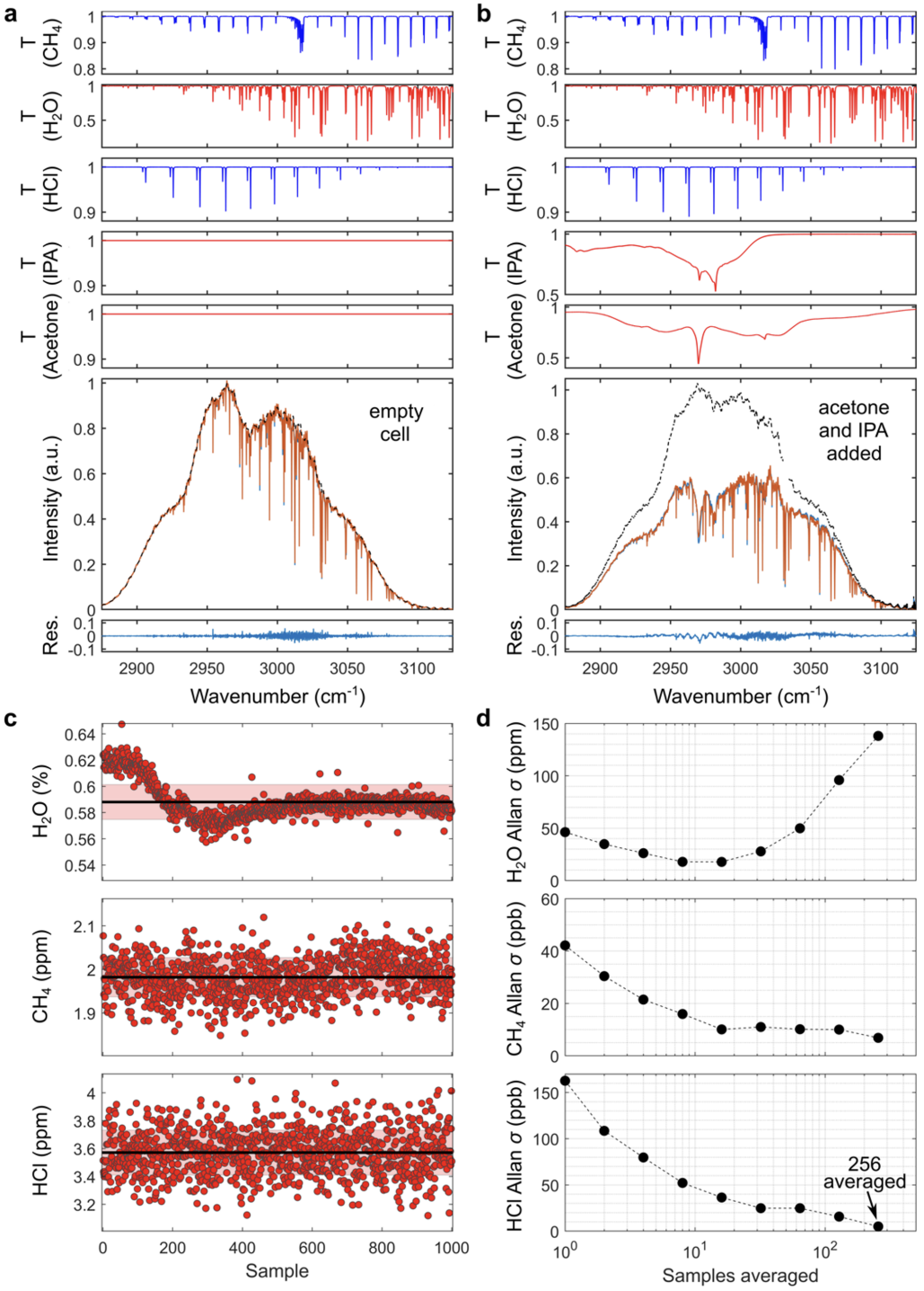

Fig. 3. (a) Average of 200 spectra acquired from a gas cell containing ambient air (red), compared to the best-fit reference spectrum (blue) for water, methane, and HCl (with naturally occurring $H^{35}Cl$ and $H^{37}Cl$ fraction). The co-fitted illumination envelope is shown by the dashed line. The fitted contributions from each species are plotted as transmission (T) spectra above the main plot. The residual is shown below, with most of the variance due to small line-shape fitting errors. (b) Equivalent fitting results when acetone and isopropanol (IPA) were introduced into the Herriott cell. (c) Concentration data resulting from 1000 independent fits to spectra acquired consecutively at 6s intervals, and (d) corresponding Allan deviations.

Optics EXPRESS

The concentrations recovered for H_2O, HCl and CH_4 remained consistent with the measurements shown in Fig. 3(a). This shows that multi-species gas spectroscopy, including a mixture of species with line-like and broad absorptions, is possible using this HCF delivery method, even in the presence of undesirable HCl absorption lines. Furthermore, up until now, mid-IR gas sensing using gas-light interaction inside HCFs has been demonstrated for only single [6–11] and dual [12] gas species detection. The measurements here highlight the potential of HCFs for sensitive mid-IR intra-fiber measurements on complex gas mixtures. While we do not actively fill the fiber with a specified gas mixture, the high level of precision demonstrated using the combination of a broadband, high brightness OPO, long lengths of low-loss HCF, and a multi-species spectral fitting algorithm shows the promise of our approach for simultaneous, multi-species gas detection using HCFs.

5. Spectroscopic measurements at tens of meters length

For sub-surface applications (e.g., in oil wells or along pipes) the fiber lengths required for remote sensing will be substantially longer than the 4.5 m demonstrated in Section 4. The absorption features observed due to in-fiber absorption at fiber lengths of a few meters are considerably more severe at lengths of tens of meters and could potentially impact the useable spectral range offered by the HCF. Expanding upon the loss measurement shown in Fig. 1, we investigated the nature of the molecular absorptions using a similar spectroscopic approach to that described in Section 4. Using the 63-meter length of HCF we recorded spectra immediately before and after the fiber (Fig. 2, detectors *b* and *c*), yielding the spectroscopy data shown Figs. 4(a) and 4(b) respectively.

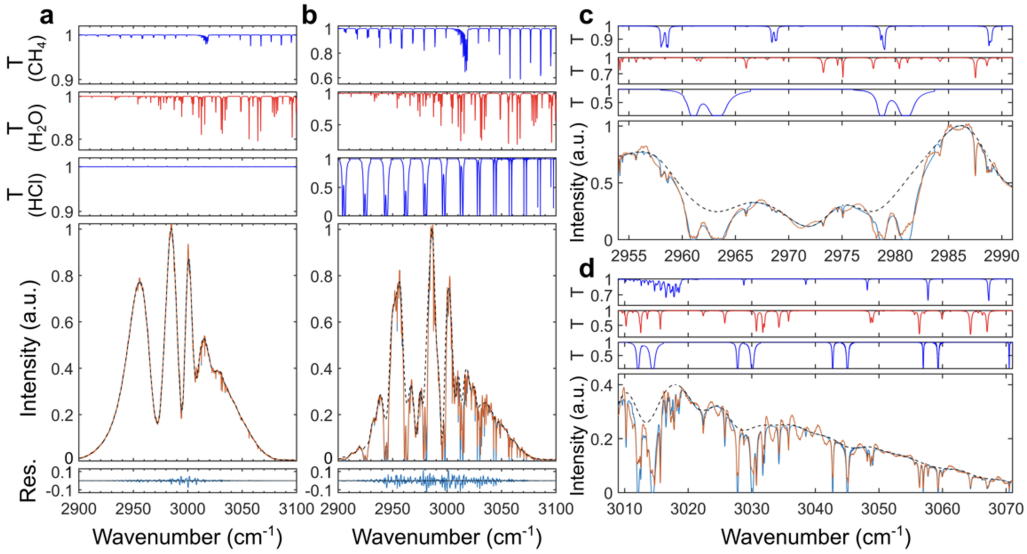

Fig. 4. Spectra from the OPO measured at the entrance (a) and exit (b) of a 63-meter length of hollow-core fiber. The measurements are the average of 16 spectra. In both cases, simultaneous fitting is carried out for $H^{37}Cl$, $H^{35}Cl$, H_2O and CH_4 (isotopologues of HCl are fitted together in their naturally occurring abundance). Water and methane in the air path from the OPO to the entrance of the fiber account for the small absorptions recorded in (a). Details of the fitted features in (b) are shown in (c) and (d).

The results in Fig. 4 show fitting for for $H^{37}Cl$, $H^{35}Cl$, H_2O and CH_4. As expected, water (H_2O) and methane (CH_4) are naturally occurring in the atmosphere at concentrations of around 0.1–1% and 2 ppm respectively, so the spectrum of the light before the fiber (Fig. 4(a)) contains small absorption features associated with the air path travelled by light from the OPO to the fiber

Optics EXPRESS

input. Inside the HCF, strong absorption is observed from $H^{37}Cl$ and $H^{35}Cl$, present in their naturally occurring isotopic fractions of 24% and 76% respectively. Saturation broadening causes the HCl lines to deplete portions of the whole spectral envelope, since at the HCl line centers the light is almost completed attenuated after the 63-m intra-fiber path. Figures 4(c) and 4(d) present details of the spectrum in Fig. 4(b), showing a region of strong HCl absorption (Fig. 4(c)) and another of lower HCl absorption (Fig. 4(d)). In both of these spectra it is easy to resolve narrow absorption features from methane and water (also present from in-fiber absorption), for example methane at 2958 cm^{-1} (Fig. 4(c)) and both species from 3055–3060 cm^{-1} (Fig. 4(d)).

This observation means that over longer fiber lengths HCF has potential to be used as a delivery fiber for subsequent hydrocarbon spectroscopy at the distal end, in a manner similar to the arrangement presented in Section 4, even without any post-processing of the HCF. For detection of a wider range of gas species, steps may be taken to remove unwanted absorption from gas species contained in the hollow core. For example, purging of the HCF with an inert gas (e.g. Argon) has been demonstrated (e.g., [3]) as an effective technique to significantly reduce or eliminate in-fiber gas absorption. Additionally, the presence of HCl can be avoided by using a chlorine-free glass as the raw material in HCF fabrication [14]. However, here we have shown that even without these additional measures, mid-IR HCFs have significant potential for light delivery for remote sensing over long fiber lengths.

6. Conclusions

Two significant findings are demonstrated by the results presented here. Firstly, a pilot measurement using short lengths of HCF demonstrated how remote spectroscopy can be implemented in which mid-IR light is delivered using HCF. Concentrations of four line-like absorbers in the free-space and fiber delivery paths were simultaneously fitted along with those of two broadband absorbers contained in a gas cell after the HCF. Critically, this proof-of-principle measurement shows successful remote spectroscopy conducted by a suitable combination of a high-brightness source, exceptional spectral resolution (sub-0.05 cm^{-1}), low loss and wide transmission fiber and a broadband spectroscopy protocol. Furthermore, it is important to note that this remote spectroscopy was possible even in the presence of in-fiber absorption due to species such as water and HCl.

Secondly, the potential of HCFs to serve as delivery channels for broadband mid-infrared light has been established by the first high-resolution transmission measurement over significant distance in this spectral region. Extending previously reported measurements [2,3,4,15], we have shown high-resolution spectroscopy which establishes directly that low-loss spectral windows exist across the 3.0–3.8-μm (2630–3333 cm^{-1}) region occupied by absorptions in hydrocarbons and other organic compounds. The transmission loss in these windows is as low as 0.1 dB m^{-1}, implying that remote spectroscopy over lengths of >100 m should be viable, opening up potential venues for HCF remote spectroscopy in sub-surface applications, structural health monitoring and distributed gas sensing. We also note the potential to fabricate HCFs from low-chlorine-content glass [14], or potentially to purge the fiber [3], which could extend the delivery range even further.

Funding. Royal Academy of Engineering; Royal Society; Engineering and Physical Sciences Research Council (EP/P030181/1); Science and Technology Facilities Council (ST/T000635/1).

Disclosures. The authors declare no conflicts of interest.

Data availability. Data supporting the results in this paper may be obtained from the authors on request.

References

1. A. N. Kolyadin, A. F. Kosolapov, A. D. Pryamikov, A. S. Biriukov, V. G. Plotnichenko, and E. M. Dianov, "Light transmission in negative curvature hollow core fiber in extremely high material loss region," Opt. Express **21**(8), 9514 (2013).
2. F. Yu, W. J. Wadsworth, and J. C. Knight, "Low loss silica hollow core fibers for 3-4 μm spectral region," Opt. Express **20**(10), 11153 (2012).

Optics EXPRESS

3. N. V. Wheeler, A. M. Heidt, N. K. Baddela, E. N. Fokoua, J. R. Hayes, S. R. Sandoghchi, F. Poletti, M. N. Petrovich, and D. J. Richardson, "Low-loss and low-bend-sensitivity mid-infrared guidance in a hollow-core-photonic-bandgap fiber," Opt. Lett. **39**(2), 295 (2014).
4. F. Yu, P. Song, D. Wu, T. Birks, D. Bird, and J. Knight, "Attenuation limit of silica-based hollow-core fiber at mid-IR wavelengths," APL Photonics **4**(8), 080803 (2019).
5. T. Ritari, J. Tuominen, H. Ludvigsen, J. C. Petersen, T. Sørensen, T. P. Hansen, and H. R. Simonsen, "Gas sensing using air-guiding photonic bandgap fibers," Opt. Express **12**(17), 4080 (2004).
6. N. Gayraud, Ł. W. Kornaszewski, J. M. Stone, J. C. Knight, D. T. Reid, D. P. Hand, and W. N. MacPherson, "Mid-infrared gas sensing using a photonic bandgap fiber," Appl. Opt. **47**(9), 1269 (2008).
7. M. N. Petrovich, A. M. Heidt, N. V. Wheeler, N. K. Baddela, and D. J. Richardson, "High sensitivity methane and ethane detection using low-loss mid-IR hollow-core photonic bandgap fibers," *23rd International Conference on Optical Fibre Sensors* (2014).
8. P. Jaworski, K. Krzempek, G. Dudzik, P. J. Sazio, and W. Belardi, "Nitrous oxide detection at 5.26 μm with a compound glass antiresonant hollow-core optical fiber," Opt. Lett. **45**(6), 1326 (2020).
9. K. Krzempek, K. Abramski, and M. Nikodem, "Kagome Hollow Core Fiber-Based Mid-Infrared Dispersion Spectroscopy of Methane at Sub-ppm Levels," Sensors **19**(15), 3352 (2019).
10. M. Nikodem, K. Krzempek, G. Dudzik, and K. Abramski, "Hollow core fiber-assisted absorption spectroscopy of methane at 3.4 μm," Opt. Express **26**(17), 21843 (2018).
11. M. Nikodem, G. Gomółka, M. Klimczak, D. Pysz, and R. Buczyński, "Demonstration of mid-infrared gas sensing using an anti-resonant hollow core fiber and a quantum cascade laser," Opt. Express **27**(25), 36350 (2019).
12. P. Jaworski, P. Kozioł, K. Krzempek, D. Wu, F. Yu, P. Bojęś, G. Dudzik, M. Liao, K. Abramski, and J. Knight, "Antiresonant Hollow-Core Fiber-Based Dual Gas Sensor for Detection of Methane and Carbon Dioxide in the Near- and Mid-Infrared Regions," Sensors **20**(14), 3813 (2020).
13. C. Yao, S. Gao, Y. Wang, P. Wang, W. Jin, and W. Ren, "Silica Hollow-Core Negative Curvature Fibers Enable Ultrasensitive Mid-Infrared Absorption Spectroscopy," J. Lightwave Technol. **38**(7), 2067–2072 (2020).
14. J. K. Lyngsø, C. Jakobsen, J. S. Gretlund, and H. R. Simonsen, "Optical fiber with improvements relating to loss and its use, method of its production and use thereof," U.S. patent application 20100266251 A1 (Oct. 21, 2010).
15. J. K. Lyngsø, B. J. Mangan, C. Jakobsen, and P. J. Roberts, "7-cell core hollow-core photonic crystal fibers with low loss in the spectral region around 2 μm," Opt. Express **17**(26), 23468 (2009).
16. G. T. Jasion, J. R. Hayes, N. V. Wheeler, Y. Chen, T. D. Bradley, D. J. Richardson, and F. Poletti, "Fabrication of tubular anti-resonant hollow core fibers: modelling, draw dynamics and process optimization," Opt. Express **27**(15), 20567 (2019).
17. O. Kara, F. Sweeney, M. Rutkauskas, C. Farrell, C. G. Leburn, and D. T. Reid, "Open-path multi-species remote sensing with a broadband optical parametric oscillator," Opt. Express **27**(15), 21358 (2019).
18. K. Johnson, P. Castro-Marin, O. Kara, C. Farrell, and D. T. Reid, "High resolution ZrF_4-fiber-delivered multi-species infrared spectroscopy," OSA Continuum **3**(12), 3595 (2020).
19. O. Kara, L. Maidment, T. Gardiner, P. G. Schunemann, and D. T. Reid, "Dual-comb spectroscopy in the spectral fingerprint region using OPGaP optical parametric oscillators," Opt. Express **25**(26), 32713 (2017).
20. M. Rutkauskas, M. Asenov, S. Ramamoorthy, and D. T. Reid, "Autonomous multi-species environmental gas sensing using drone-based Fourier-transform infrared spectroscopy," Opt. Express **27**(7), 9578 (2019).
21. E. Gordon, L. S. Rothman, C. Hill, R. V. Kochanov, Y. Tan, P. F. Bernath, M. Birk, V. Boudon, A. Campargue, K. V. Chance, B. J. Drouin, J.-M. Flaud, R. R. Gamache, J. T. Hodges, D. Jacquemart, V. I. Perevalov, A. Perrin, K. P. Shine, M.-A. H. Smith, J. Tennyson, G. C. Toon, H. Tran, V. G. Tyuterev, A. Barbe, A. G. Császár, V. M. Devi, T. Furtenbacher, J. J. Harrison, J.-M. Hartmann, A. Jolly, T. J. Johnson, T. Karman, I. Kleiner, A. A. Kyuberis, J. Loos, O. M. Lyulin, S. T. Massie, S. N. Mikhailenko, N. Moazzen-Ahmadi, H. S. P. Müller, O. V. Naumenko, A. V. Nikitin, O. L. Polyansky, M. Rey, M. Rotger, S. W. Sharpe, K. Sung, E. Starikova, S. A. Tashkun, J. V. Auwera, G. Wagner, J. Wilzewski, P. Wcisło, S. Yu, and E. J. Zak, "The HITRAN2016 molecular spectroscopic database," J. Quant. Spectrosc. Radiat. Transfer **203**, 3–69 (2017).
22. R. V. Kochanov, I. E. Gordon, L. S. Rothman, P. Wcisło, C. Hill, and J. S. Wilzewski, "HITRAN Application Programming Interface (HAPI): A comprehensive approach to working with spectroscopic data," J. Quant. Spectrosc. Radiat. Transfer **177**, 15–30 (2016).
23. S. W. Sharpe, T. J. Johnson, R. L. Sams, P. M. Chu, G. C. Rhoderick, and P. A. Johnson, "Gas-phase databases for quantitative infrared spectroscopy," Appl. Spectrosc. **58**(12), 1452–1461 (2004).